

Chemistry of the Oxophosphinidene Ligand. 2. Reactivity of the Anionic Complexes $[\text{MCp}\{\text{P}(\text{O})\text{R}^*\}(\text{CO})_2]^-$ ($\text{M} = \text{Mo}, \text{W}$; $\text{R}^* = 2,4,6\text{-C}_6\text{H}_2^t\text{Bu}_3$) Toward Electrophiles Based on Elements Different from Carbon.

María Alonso, M. Angeles Alvarez, M. Esther García,* Miguel A. Ruiz,* Hayrullo Hamidov,[†] and John C. Jeffery[†]

Departamento de Química Orgánica e Inorgánica/IUQOEM, Universidad de Oviedo, 33071 Oviedo, Spain, and

[†]School of Chemistry, University of Bristol, Bristol BS8 1TS, U.K.

Received September 7, 2010

The anionic oxophosphinidene complexes $(\text{H-DBU})[\text{MCp}\{\text{P}(\text{O})\text{R}^*\}(\text{CO})_2]$ ($\text{M} = \text{Mo}, \text{W}$; $\text{R}^* = 2,4,6\text{-C}_6\text{H}_2^t\text{Bu}_3$; $\text{Cp} = \eta^5\text{-C}_5\text{H}_5$, $\text{DBU} = 1,8\text{-diazabicyclo}[5.4.0]\text{ undec-7-ene}$) displayed multisite reactivity when faced with different electrophilic reagents. The reactions with the group 14 organochloride compounds $\text{ER}_{4-x}\text{Cl}_x$ ($\text{E} = \text{Si}, \text{Ge}, \text{Sn}, \text{Pb}$) led to either phosphide-like, oxophosphinidene-bridged derivatives $[\text{MCp}\{\text{P}(\text{OE}')\text{R}^*\}(\text{CO})_2]$ ($\text{E}' = \text{SiMe}_3, \text{SiPh}_3, \text{GePh}_3, \text{GeMe}_2\text{Cl}$) or to terminal oxophosphinidene complexes $[\text{MCp}\{\text{P}(\text{O})\text{R}^*\}(\text{CO})_2(\text{E}')]^-$ ($\text{E}' = \text{SnPh}_3, \text{SnPh}_2\text{Cl}, \text{PbPh}_3$; $\text{Mo-Pb} = 2.8845(4)$ Å for the MoPb compound). A particular situation was found in the reaction with SnMe_3Cl , this giving a product existing in both tautomeric forms, with the phosphide-like complex $[\text{MCp}\{\text{P}(\text{OSnMe}_3)\text{R}^*\}(\text{CO})_2]$ prevailing at room temperature and the tautomer $[\text{MCp}\{\text{P}(\text{O})\text{R}^*\}(\text{CO})_2(\text{SnMe}_3)]^-$ being the unique species present below 203 K in dichloromethane solution. The title anions also showed a multisite behavior when reacting with transition-metal based electrophiles. Thus, the reactions with the complexes $[\text{M}'\text{Cp}_2\text{Cl}_2]$ ($\text{M}' = \text{Ti}, \text{Zr}$) gave phosphide-like derivatives $[\text{MCp}\{\text{P}(\text{OM}')\text{R}^*\}(\text{CO})_2]$ ($\text{M} = \text{Mo}, \text{M}' = \text{TiCp}_2\text{Cl}, \text{ZrCp}_2\text{Cl}$; $\text{M} = \text{W}, \text{M}' = \text{ZrCp}_2\text{Cl}$), displaying a bridging $\kappa^1, \kappa^1\text{-P}_2\text{O}$ -oxophosphinidene ligand connecting $\text{MCp}(\text{CO})_2$ and $\text{M}'\text{Cp}_2\text{Cl}$ metal fragments ($\text{W-P} = 2.233(1)$ Å, $\text{O-Zr} = 2.016(4)$ Å for the WZr compound). In contrast, the reactions with the complex $[\text{AuCl}\{\text{P}(\text{p-tol})_3\}]$ gave the metal–metal bonded derivatives *trans*- $[\text{MCp}\{\text{P}(\text{O})\text{R}^*\}(\text{CO})_2\{\text{AuP}(\text{p-tol})_3\}]^-$ ($\text{M} = \text{Mo}, \text{W}$; $\text{Mo-Au} = 2.7071(7)$ Å). From all the above results it was concluded that the terminal oxophosphinidene complexes are preferentially formed under conditions of orbital control, while charge-controlled reactions tend to give derivatives with the electrophilic fragment bound to the oxygen atom of the oxophosphinidene ligand (phosphide-like, oxophosphinidene-bridged derivatives).

Introduction

Oxophosphinidenes (R-P=O) are unstable molecules of relevance as intermediates in the synthesis of different organophosphorus products.^{1,2} They can be isolobally-related to the electrophilic carbenes,³ and thus might be expected to act as ligands to many very different metal fragments. However, in spite of the rich variety of coordination modes available for these molecules, only a very limited number of complexes have been described in the literature so far,⁴ and their chemical behavior has not been explored.

In the context of our studies on the chemistry of binuclear phosphinidene complexes of the transition metals, we recently found a selective synthetic route to the molybdenum compound $(\text{H-DBU})[\text{MoCp}\{\text{P}(\text{O})\text{R}^*\}(\text{CO})_2]$ (**1**), the first anionic oxophosphinidene complex reported in the literature.^{5a} Our preliminary experiments revealed that the expectedly high nucleophilicity of this complex would open

*To whom correspondence should be addressed. E-mail: mara@uniovi.es (M.A.R.).

(1) (a) Gaspar, P. P.; Qian, H.; Beatty, A. M.; d'Avignon, D. A.; Kao, J. L.-F.; Watt, J. C.; Rath, N. P. *Tetrahedron* **2000**, *56*, 105. (b) Cowley, A. H.; Gabbai, F. P.; Corbelin, S.; Decken, A. *Inorg. Chem.* **1995**, *34*, 5931. (c) Wang, K.; Emge, T. J.; Goldman, A. S. *Organometallics* **1994**, *13*, 2135.

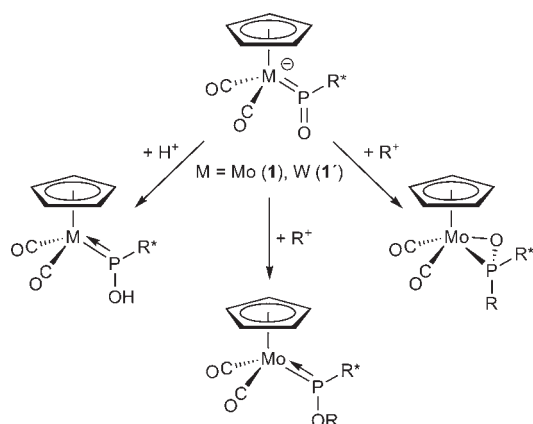
(2) (a) Stille, J. K.; Eichelberger, J. L.; Higgins, J.; Freeburger, M. E. *J. Am. Chem. Soc.* **1972**, *94*, 4761. (b) Nakayama, S.; Yoshifuji, M.; Okazaki, R.; Inamoto, N. *Bull. Chem. Soc. Jpn.* **1975**, *48*, 546. (c) Quast, H.; Heuschmann, M. *Angew. Chem., Int. Ed. Engl.* **1978**, *17*, 867. (d) Quin, L. D.; Yao, E. U.; Szweczyk, J. *Tetrahedron Lett.* **1987**, *28*, 1077.

(3) Schoeller, W. W.; Niecke, E. *J. Chem. Soc., Chem. Commun.* **1982**, 569.

(4) (a) Niecke, E.; Engelmann, M.; Zorn, H.; Krebs, B.; Henkel, G. *Angew. Chem., Int. Ed. Engl.* **1980**, *19*, 710. (b) Hitchcock, P. B.; Johnson, J. A.; Lemos, M. A. N. D. A.; Meidine, M. F.; Nixon, J. F.; Pombeiro, A. J. L. *J. Chem. Soc., Chem. Commun.* **1992**, 645. (c) Alvarez, M. A.; García, M. E.; González, R.; Ramos, A.; Ruiz, M. A. *Organometallics* **2010**, *29*, 1875. (d) Johnson, M. J. A.; Odom, A. L.; Cummins, C. C. *J. Chem. Soc., Chem. Commun.* **1997**, 1523. (e) Kourkine, V.; Glueck, D. S. *Inorg. Chem.* **1997**, *36*, 5160. (f) Schmitt, G.; Ullrich, D.; Wolmershäuser, G.; Regitz, M.; Scherer, O. J. *Z. Anorg. Allg. Chem.* **1999**, *625*, 702. (g) Alvarez, C. M.; Alvarez, M. A.; García, M. E.; González, R.; Ruiz, M. A. *Organometallics* **2005**, *24*, 5503. (h) Buchholz, D.; Huttner, G.; Imhof, W. *J. Organomet. Chem.* **1990**, *388*, 307.

(5) (a) Alonso, M.; García, M. E.; Ruiz, M. A.; Hamidov, H.; Jeffery, J. C. *J. Am. Chem. Soc.* **2004**, *126*, 13610. (b) Alonso, M.; Alvarez, M. A.; García, M. E.; Ruiz, M. A.; Hamidov, H.; Jeffery, J. C. *J. Am. Chem. Soc.* **2005**, *127*, 15012. (c) Alonso, M.; Alvarez, M. A.; García, M. E.; Ruiz, M. A. *Inorg. Chem.* **2008**, *47*, 1252.

Scheme 1



the way to explore at a great extent the reactivity of the metal-bound oxophosphinidene ligand,^{5a-c} and we then decided to study in detail the chemical behavior of this anion. In the first full report of this wide study, we analyzed the reactivity of the above molybdenum complex and that of its tungsten analogue (H-DBU)[WCp{P(O)R*}(CO)₂] (**1'**) toward several protic acids and C-based electrophiles (Scheme 1).⁶

Thus we found that these anionic complexes were easily protonated at the O atom of the oxophosphinidene ligand to give the hydroxyphosphide derivatives [MCp{P(OH)R*}(CO)₂], and that the molybdenum anion reacted analogously with strong C-based electrophiles to give the corresponding alkoxyphosphide derivatives [MoCp{P(OR)R*}(CO)₂]. In contrast, the reactions with milder alkylating reagents gave selectively the corresponding κ^2 -phosphinite complexes [MoCp{ κ^2 -OP(R)R*}(CO)₂], as a result of the attack of the electrophile at the P atom of the oxophosphinidene ligand. According to density functional theory (DFT) calculations on the Mo anion, the oxygen atom of the phosphinidene ligand bears the highest negative charge of the molecule, while the highest occupied molecular orbital (HOMO) of this complex has substantial Mo–P π bonding character. Thus, it was concluded that the phosphinite complexes are formed under conditions of orbital control, while charge-controlled reactions tend to give alkoxyphosphide derivatives.⁶

In this paper we analyze the reactivity of the anions **1** and **1'** toward several electrophilic reagents based on elements different from carbon, either the heavier group 14 elements (Si to Pb) or some transition and post-transition metals (Ti, Zr, Au, Ag). As it will be discussed, these reactions may involve the binding of the electrophilic fragment to either the O atom of the oxophosphinidene ligand or the metal atom, thus leading to κ^1, κ^1 -P,O-bridged or terminal oxophosphinidene complexes, respectively. While the former reactions are reminiscent of the formation of alkoxyphosphide complexes mentioned above, no derivatives involving the attachment of the electrophile to the P atom of the oxophosphinidene ligand have been observed in the reactions now reported.

Results and Discussion

Reactions of Compounds 1 and 1' with ER_{4-x}Cl_x (E = Si to Pb). The anionic complexes **1** and **1'** react rapidly at 273 K

Scheme 2

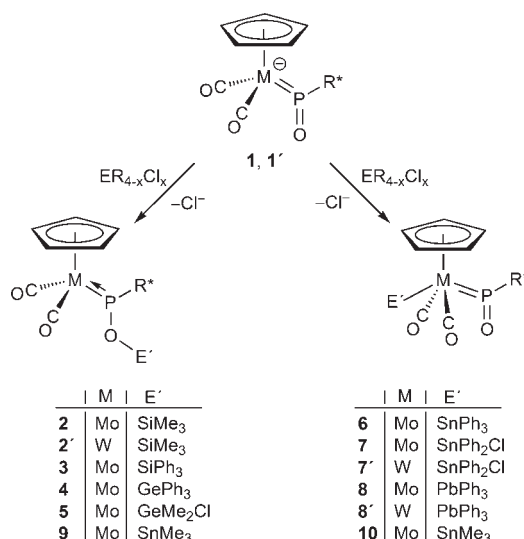
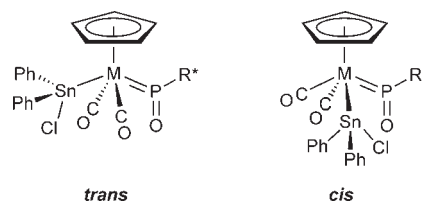


Chart 1



or room temperature with different organohalide compounds ER_{4-x}Cl_x ($x = 1, 2$) of the group 14 elements to give derivatives with terminal or bridging oxophosphinidene ligands depending on the site of attachment (M or O) of the electrophilic fragment (Scheme 2).

Thus the reactions with SiR₃Cl (R = Ph, Me) give the corresponding silyloxyphosphide derivatives [MCp{P(OSiR₃)R*}(CO)₂] (M = Mo, R = Me (**2**), Ph (**3**); M = W, R = Me (**2'**)). In a similar way, compound **1** reacts with GePh₃Br or GeMe₂Cl₂ at 273 K to give the corresponding derivatives [MoCp{P(OE)R*}(CO)₂] (E = GePh₃ (**4**), GeMe₂Cl (**5**)), the process being faster for GeMe₂Cl₂. These reactions are reminiscent of the formation of alkoxyphosphide complexes in the reactions of **1** with strong C-based electrophiles,⁶ and they might analogously be interpreted as favored on electrostatic grounds (charge control).

In contrast, the reactions of **1** with SnPh₃Cl, SnPh₂Cl₂, and PbPh₃Cl, that is, with electrophiles based on the softer members of the group 14 elements, give instantaneously the metal–metal bonded complexes [MoCp{P(O)R*}(CO)₂(SnPh₃)] (**6**), [MoCp{P(O)R*}(CO)₂(SnPh₂Cl)] (**7**), and [MoCp{P(O)R*}(CO)₂(PbPh₃)] (**8**), respectively, all of them retaining a terminal oxophosphinidene ligand. In the same line, the tungsten compound **1'** reacts with SnPh₂Cl₂ and PbPh₃Cl to give the corresponding heterometallic derivatives [WCp{P(O)R*}(CO)₂(SnPh₂Cl)] (**7'**) and [WCp{P(O)R*}(CO)₂(PbPh₃)] (**8'**), respectively (Scheme 2). The synthesis of the molybdenum–tin compounds **6** and **7** was described in our preliminary reports on the chemistry of the oxophosphinidene ligand,^{5a,c} with the latter complex displaying a remarkable hydrolytic behavior.^{5c} Moreover, we note here that while the SnPh₃ and PbPh₃

(6) Alonso, M.; Alvarez, M. A.; García, M. E.; García-Vivó, D.; Ruiz, M. A. *Inorg. Chem.* **2010**, *49*, 8962.

Table 1. IR and $^{31}\text{P}\{^1\text{H}\}$ NMR Data for Compounds **2** to **10**

compound	$\nu_{\text{st}}(\text{CO})^a/\text{cm}^{-1}$	$\delta_{\text{P}}/\text{ppm}^b [J_{\text{PW}}], (J_{119\text{SnP}}), \{J_{117\text{SnP}}\}/\text{Hz}$
[MoCp{P(OSiMe ₃)R*}(CO) ₂] (2)	1934 (vs), 1854 (s)	319.3 ^c
[WCp{P(OSiMe ₃)R*}(CO) ₂] (2')	1924 (vs), 1842 (s)	272.4 [735]
[MoCp{P(OSiPh ₃)R*}(CO) ₂] (3)	1940 (vs), 1858 (s)	306.9 ^c
[MoCp{P(OGePh ₃)R*}(CO) ₂] (4)	1930 (vs), 1850 (s)	330.6
[MoCp{P(OGeMe ₂ Cl)R*}(CO) ₂] (5)	1935 (vs), 1854 (s)	333.8
[MoCp{P(O)R*}(CO) ₂ (SnPh ₃)] (6)	1947 (m), 1889 (vs)	468.1(116){116} ^e
[MoCp{P(O)R*}(CO) ₂ (SnPh ₂ Cl)] (7)	2001(m), 1960 (s), 1899 (vs) ^a 1999 (vs), 1960 (s), 1906 (s) ^d	<i>trans</i> : 475.3 (149){149} <i>cis</i> : 438.5 (540){516}
[WCp{P(O)R*}(CO) ₂ (SnPh ₂ Cl)] (7')	1994 (m), 1952 (s), 1891 (vs) ^a 1993 (vs), 1950 (s), 1901 (m) ^d	<i>trans</i> : 420.2 [372]{147}{147} <i>cis</i> : 376.0 [422]{548}{530}
[MoCp{P(O)R*}(CO) ₂ (PbPh ₃)] (8)	1949 (m), 1893 (vs)	467.5 ($J_{\text{PPb}} = 177$)
[WCp{P(O)R*}(CO) ₂ (PbPh ₃)] (8')	1944 (m), 1885 (vs)	412.4 [393], ($J_{\text{PPb}} = 168$)
[MoCp{P(OSnMe ₃)R*}(CO) ₂] (9)	1913 (vs), 1831 (s)	350.7 ^e
[MoCp{P(O)R*}(CO) ₂ (SnMe ₃)] (10)		458.0 ^f

^a Recorded in dichloromethane solution, unless otherwise stated. ^b Recorded in CD₂Cl₂ solution at 290 K and 121.50 MHz unless otherwise stated; δ relative to external 85% aqueous H₃PO₄. ^c Recorded at 81.03 MHz. ^d Recorded in petroleum ether solution. ^e Recorded in C₆D₆ solution at 290 K and 81.03 MHz. ^f Recorded in CD₂Cl₂ solution at 203K and 162.14 MHz.

products are obtained as single (*trans*) isomers, the SnPh₂Cl products are obtained as an equilibrium mixture of *cis* and *trans* isomers (Chart 1), a matter to be discussed later on.

The subtle effects of the substituents present in the added electrophile can even counterbalance the formation of one or another type of products in the above reactions, as suggested by the nature the SnMe₃ derivative of compound **1**, that at room temperature exists mainly in its oxophosphinidene-bridged form [MoCp{P(OSnMe₃)R*}-(CO)₂] (**9**), but in its terminal form [MoCp{P(O)R*}-(CO)₂(SnMe₃)] (**10**) below 203 K. Although we have not observed this sort of equilibrium for other complexes in this work, we cannot exclude that similar processes may take place to a very small extent in other cases, and this leads us to think that the type of structure actually displayed by compounds **2** to **10** is not kinetically, but thermodynamically governed.

Structural Characterization of Compounds 2–5 and 9. Spectroscopic data in solution for compounds **2–5**, **2'**, and **9** are comparable to each other (Table 1 and Experimental Section) and to those of the structurally characterized complexes [MoCp(PFR*)(CO)₂] and [MoCp{P(OC(O)Ph)R*}(CO)₂],⁶ supporting the presence of an oxophosphinidene ligand bridging the Mo/W and Si/Ge/Sn atoms in these molecules, and keeping a planar trigonal environment around the P atom. The latter atom then formally behaves as a 3-electron donor to the Mo/W atom (alkoxyphosphide-like coordination). Moreover, these data are also similar to those reported for comparable phosphide complexes having a supermesityl substituent, such as [MCp(PHR*)(CO)₂] and [MCp(PClR*)(CO)₂] (M = Mo, W),⁷ and to those for the hydroxyphosphide derivatives of **1** and **1'**, [MoCp{P(OH)R*}(CO)₂] and [WCp{P(OH)R*}(CO)₂],⁶ indicating that all those molecules share the same basic structure. The P-donor ligand in these compounds gives rise to quite deshielded ^{31}P resonances, in the range 270–350 ppm, a feature explained by the combination of two effects of known deshielding influence on P-donor ligands, the presence of oxygen bound to phosphorus, and the multiple nature

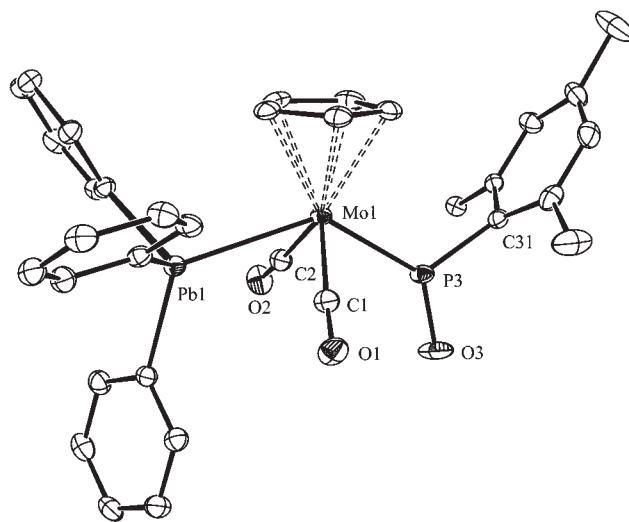


Figure 1. ORTEP drawing (30% probability) of the molecular structure of compound **8**, with all H atoms and Me groups omitted for clarity.

of the metal–phosphorus bond,⁸ with the latter leading to a diminished HOMO–LUMO gap and hence to an increased paramagnetic contribution to the phosphorus shielding. This also justifies the fact that our complexes display ^{31}P chemical shifts substantially higher than those of the mentioned complexes [MoCp(PXR*)(CO)₂] (X = H (266.2 ppm), Cl (259.1 ppm)),⁷ and within the range found for the alkoxyphosphide complexes [MoCp{P(OR)R*}-(CO)₂] (290–350 ppm for R = Me, Et, COC₂H₅, CPh).⁶ In addition, the ^{31}P NMR spectrum of the tungsten complex **2'** exhibits a quite large ^{31}P – ^{183}W coupling of 735 Hz, comparable to that measured in the hydroxyphosphide complex [WCp{P(OH)R*}(CO)₂] ($J_{\text{PW}} = 704$ Hz),⁶ with these values being consistent with the formulation of double W–P bonds for these molecules.⁹

Solid-State Structure of Compound 8. The molecule of the dicarbonyl complex **8** in the crystal (Figure 1 and Table 2) displays a distorted four-legged piano stool

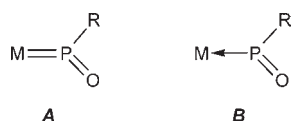
(7) Malisch, W.; Hirth, U.-A.; Grün, K.; Schmeuber, M. *J. Organomet. Chem.* **1999**, *572*, 207.

(8) Carty, A. J.; MacLaughlin, S. A.; Nucciarone, D. In *Phosphorus-31 NMR Spectroscopy in Stereochemical Analysis*; Verkade, J. G., Quin, L. D., Eds.; VCH: Deerfield Beach, FL, 1987; Chapter 16.

(9) (a) Lambert, J. A.; Mazzola, E. P. *Nuclear Magnetic Resonance. An Introduction to Principles and Experimental Methods*; Pearson: London, 2003. (b) Jameson, C. J. In *Phosphorus-31 NMR Spectroscopy in Stereochemical Analysis*; Verkade, J. G., Quin, L. D., Eds.; VCH: Deerfield Beach, FL, 1987; Chapter 6.

Table 2. Selected Bond Lengths (Å) and Angles (deg) in Compound **8**

Mo(1)–P(3)	2.319(1)	Mo(1)–C(1)	1.983(5)
Mo(1)–Pb(1)	2.8845(4)	Mo(1)–C(2)	1.987(5)
P(3)–O(3)	1.482(3)	P(3)–C(31)	1.838(4)
C(1)–Mo(1)–C(2)	102.0(2)	C(111)–Pb(1)–Mo(1)	106.1(1)
O(3)–P(3)–C(31)	113.0(2)	C(121)–Pb(1)–Mo(1)	118.1(1)
O(3)–P(3)–Mo(1)	130.1(2)	C(101)–Pb(1)–Mo(1)	111.1(1)
C(31)–P(3)–Mo(1)	116.8(1)	C(111)–Pb(1)–C(121)	108.6(2)
P(3)–Mo(1)–Pb(1)	132.6(1)	C(111)–Pb(1)–C(101)	103.9(2)
O(1)–C(1)–Mo(1)	176.2(4)	C(121)–Pb(1)–C(101)	108.1(2)
O(2)–C(2)–Mo(1)	175.5(4)		

Chart 2

structure, with the PbPh_3 and oxophosphinidene groups in *trans* arrangement. The Mo–P length of 2.319 (1) Å is substantially shorter than the values of about 2.45 Å characteristic of single Mo–P bonds (e.g., those in Mo(II) phosphine complexes), but about 0.08 Å longer than the one measured in the anion **1** (2.238(1) Å), and substantially longer than other reference figures for double Mo–P bonds, such as the values of about 2.20 Å for the complexes $[\text{MoCp}\{\text{P}(\text{X})\text{R}^*\}(\text{CO})_2]$ (X = F, C(O)Ph),⁶ or the very short Mo–P length of 2.1439(5) Å measured in the diphosphenide complex $[\text{Mo}(\text{N}^i\text{BuAr})_3(\text{P} = \text{PSi}^i\text{Pr}_3)]$ (Ar = 3,5-Me₂C₆H₃).¹⁰ At the same time, the P–O length in **8** (1.482(7) Å) is slightly shorter than that measured in its precursor **1** (1.514(3) Å), and is virtually identical to that measured for the double P–O bond in the terminal PO complex $[\text{Mo}(\text{N}^i\text{BuAr})_3(\text{PO})]$ (1.49(2) Å).^{4d} Thus we conclude that the metal-oxophosphinidene bonding in compound **8** is best described as an average of the extreme distributions represented by the canonical forms **A** and **B** in Chart 2. This is in contrast with the anion in compound **1**, where the Mo–P and P–O bonds can be described as essentially double bonds, and therefore might be adequately represented by just the canonical structure **A**. This difference can be understood by considering that on going from **1** to **8** there is a strong reduction of the electron density at the metal atom therefore greatly suppressing the back-donation (Mo to P) responsible for the double-bond character of the Mo–P interaction. Of course a similar situation is to be expected for the related tin complexes **7** and **10**. Interestingly, we note that the above difference concerning the nature of the Mo–P bond when going from the anion **1** to their neutral derivatives **6–8** or **10** is completely analogous to that existing between nucleophilic (P=M bonding) and electrophilic (P→M bonding) phosphinidene complexes.¹¹

In agreement with the multiplicity of the Mo–P and P–O bonds in **8**, the coordination environment around phosphorus is planar trigonal (sum of angles = 359.9°), with the Mo, P, O3, and C31 atoms contained in a plane almost bisecting the molecule, and the aryl group orientated

perpendicularly to it, as found in the precursor **1**. We should remark that the aryl group is placed specifically *cis* to the Cp ligand of the complex. This conformation around the multiple Mo–P bond is also reproduced in all derivatives of **1** as noticed previously,⁶ and is further confirmed by the present work, it likely being the most favored one on steric grounds. Concerning the geometry around the metal atom, we note that the P–Mo–Pb angle (132.6(1)°) is significantly wider than the C(1)–Mo–C(2) one (102.0(2)°). This might be in part justified on the basis of the larger steric requirements of the PbPh_3 and $\text{P}(\text{O})\text{R}^*$ groups, that would take them as far apart from each other as possible. Additionally, this distortion also follows the established pattern of *angular trans influence*,¹² which places the pair of ligands with overall stronger σ -bonding ability at smaller L–M–Cp(centroid) angles, to maximize the interaction with the more favorable metal orbitals.¹³ In the case of **8**, however, this distortion is essentially limited to the PbPh_3 group ($\text{Pb–Mo–Cp}(\text{centr.}) = 107.2^\circ$), while the oxophosphinidene ligand defines a rather normal P–Mo–Cp(cent.) angle of 120.4°, perhaps because of steric limitations. On the other hand, the Mo–Pb length of 2.8845(4) Å in **8** is only slightly below the value found in the structurally related tricarbonyl complex $[\text{Mo}(\text{PbPh}_3)\text{Cp}(\text{CO})_3]$ (Mo–Pb = 2.90 Å).¹⁴ This indicates that the *trans* influence¹⁵ of the oxophosphinidene ligand is comparable to that (strong one) of the carbonyl ligand. We finally note that, concerning the environment around the lead atom, the C–Pb–C bond angles (ca. 107°) are smaller than the Mo–Pb–C ones (ca. 112°), as expected both on steric grounds and also from the higher electronegativity of the Ph groups (compared to the Mo fragment), as predicted by the Bent model.¹⁶

Solution Structure of Compounds 6–8 and 10. The IR spectra of compounds **6**, **8**, and **8'** (Table 1) display in each case two C–O stretching bands, with relative intensities characteristic of *trans*-dicarbonyl complexes, in agreement with the structure of **8** in the crystal. These structures are therefore comparable to those of the related phosphine complexes $[\text{MoCp}(\text{SnR}_3)(\text{CO})_2\text{L}]$ (R = Me, Ph; L = PPh_3 , $\text{P}(\text{O}i\text{Pr})_3$, SbPh_3),¹⁷ and to those of the carbene complexes $[\text{MCp}(\text{M}'\text{Ph}_3)(\text{CO})_2\{\text{C}(\text{OR}')\text{R}\}]$ (M = Mo, W; M' = Ge, Sn).¹⁸ All these complexes were found to exist in solution exclusively as the corresponding *trans* isomers, although the carbene complexes displayed two conformers related by a restricted rotation of the carbene ligand around the corresponding M–C bond. In contrast, the SnPh_2Cl compounds **7** and **7'** display three C–O stretching bands, indicative of the presence of both *cis* and *trans* isomers, with their ratio being dependent on the polarity of the solvent. For instance, the IR spectrum of **7** in CH_2Cl_2 solution displays bands at 2001 (m), 1960 (s),

(12) Poli, R. *Organometallics* **1990**, *9*, 1892.(13) Lin, Z.; Hall, M. B. *Organometallics* **1993**, *12*, 19.(14) Struchkov, Y. T.; Anisimov, K. N.; Osipova, O. P.; Kolobova, N. E.; Nesmeyanov, A. N. *Dokl. Akad. Nauk. SSSR* **1967**, *172*, 107.(15) Cotton, F. A.; Wilkinson, G. *Advanced Inorganic Chemistry*, 5th ed.; Wiley: New York, 1988; p 1299.(16) Bent, H. A. *Chem. Rev.* **1961**, *61*, 275.(17) (a) Manning, A. R. *J. Chem. Soc., A* **1968**, 651. (b) George, T. A. *Inorg. Chem.* **1972**, *11*, 77.(18) (a) Dean, W. K.; Graham, W. A. G. *Inorg. Chem.* **1977**, *16*, 1061. (b) Chan, L. Y. Y.; Dean, W. K.; Graham, W. A. G. *Inorg. Chem.* **1977**, *16*, 1067.(10) Piro, N. A.; Cummins, C. C. *J. Am. Chem. Soc.* **2009**, *131*, 8764.(11) (a) Aktas, H.; Slootweg, J. C.; Lammertsma, K. *Angew. Chem., Int. Ed.* **2010**, *49*, 2. (b) Lammertsma, K. *Top. Curr. Chem.* **2003**, *229*, 95.(c) Lammertsma, K.; Vlaar, M. J. M. *Eur. J. Org. Chem.* **2002**, 1127.(d) Mathey, F.; Tran-Huy, N. H.; Marinetti, A. *Helv. Chim. Acta* **2001**, *84*, 2938.

and 1899 (vs) cm^{-1} , and their relative intensities are strongly modified when recorded in petroleum ether solution, these now appearing at 1999 (vs), 1960 (s), and 1906 (s) cm^{-1} . This indicates an increase of the relative proportion of the *cis* isomer in the latter, less polar solvent, and similar changes were observed in the IR spectra of the tungsten compound **7'** (Table 1).

Equilibria between *cis* and *trans* isomers is a common feature of complexes having a four-legged piano stool structure, and the different factors involved in this isomerism have been extensively studied, both in solution and in the solid state.^{19,20} For instance, the *cis/trans* equilibrium ratio in solution for the complexes $[\text{MoCpX}(\text{CO})_2\text{L}]$ ($\text{L} = \text{P}(\text{OMe})_3, \text{PPh}_3$), increases in the order $\text{X} = \text{I} < \text{Br} < \text{Cl}$.²⁰ The presence of bulky groups is expected to disfavor somewhat the *cis* isomers for dicarbonyl complexes; for instance, the complex $[\text{MoCpMe}(\text{CO})_2\text{-}\{\text{PN}(\text{MeCH}_2\text{CH}_2\text{NMe}(\text{OMe}))\}]$ displays *cis* and *trans* isomers in solution, but the related MoSn complex $[\text{MoCp}(\text{CO})_2\{\text{PN}(\text{MeCH}_2\text{CH}_2\text{NMe}(\text{OMe}))\}(\text{SnR}_3)]$ only displays the *trans* isomer.²¹ Although the steric effects do not seem to rule the *cis/trans* isomerism in these complexes,²² the smaller size of the SnPh_2Cl group (compared to that of the SnPh_3 or PbPh_3 groups) might be the relevant factor behind the appearance of the *cis* isomer just for compounds **7** and **7'**. This would be so in our compounds because, as we have discussed above, the *trans* influence of the oxophosphinidene ligand might be comparable to that of the carbonyl ligands, and therefore the electronic effects might have only a modest influence on the *cis/trans* isomerism in our complexes.

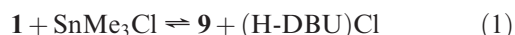
As expected, the *cis/trans* equilibrium for compounds **7** and **7'** is also solvent- and temperature-dependent. Thus, in the case of **7** the *cis* isomer is moderately favored by lowering the temperature, with the *cis/trans* ratio being increased from 2/7 at 293 K to 2/5 at 193 K. The solvent has a much stronger influence on this equilibrium and, in line with the qualitative trend deduced from the IR data mentioned above, the *cis* isomer is favored for the less polar solvent, with the *cis/trans* ratio being increased to about 3/2 in C_6D_6 solution.

The oxophosphinidene ligand in compounds **6** to **8** and **10** gives rise to a strongly deshielded resonance in the ranges 460–475 ppm (Mo) or 415–420 ppm (W) for the *trans* isomers, that is, some 80 ppm downfield from the corresponding resonance in the anionic precursors **1** (385.0 ppm) and **1'** (335.6 ppm).⁶ These shifts are also substantially higher than those measured for the complexes $[\text{Cr}(\text{CO})_5\{\text{P}(\text{O})\text{N}(\text{Pr})_2\}]$ ($\delta_{\text{P}} = 319.2$ ppm),^{4a} $[\text{ReCl}(\text{dppm})_2\{\text{P}(\text{O})\text{CH}_2\text{tBu}\}]$ (340.1 ppm)^{4b} and $[\text{Fe}_2\text{Cp}_2(\mu\text{-CO})_2(\text{CO})\{\text{P}(\text{O})\text{R}^*\}]$ (432.5 ppm),^{4c} these being the only other terminal oxophosphinidene complexes previously reported. The strong deshielding effect on the P nucleus (relative to the parent anions) might be justified

by recalling that the strong reduction of the electron density at the metal atom operated upon formation of these neutral compounds from the anions **1** and **1'** should greatly suppress the back-donation of electron density from the metal atom to P (π interaction), as noted above, and therefore should at least greatly reduce the diamagnetic contribution to the shielding of this nucleus.⁸ On the other hand, the *cis* isomers in compounds **7** and **7'** give rise to ³¹P resonances some 40 ppm below those of the corresponding *trans* isomers, a difference difficult to be justified on simple grounds.

The inspection of the metal–phosphorus couplings apparent in the ³¹P resonances of these compounds also is highly informative. Thus, the tin compounds having a *trans* geometry display relatively small two-bond ³¹P–Sn couplings (ca. 115 Hz for **6** or 150 Hz for **7** and **7'**), whereas the *cis* isomers of compounds **7** and **7'** display much higher values (ca. 550 Hz with the ¹¹⁹Sn nucleus). This difference is consistent with the general trend in the absolute values (${}^2J_{\text{cis}} > {}^2J_{\text{trans}}$) found for ${}^2J_{\text{XY}}$ in complexes of the type $[\text{MCp}(\text{CO})_2\text{XY}]$.^{9b} We also note that the tungsten compounds **7'** and **8'** display P–W couplings of about 400 Hz, almost half the value of 735 Hz measured in the silyloxyphosphide complex **2'**, but still higher than the value of 294 Hz measured for the closely related phosphine complex *trans*- $[\text{WCp}(\text{CO})_2(\text{PPh}_3)(\text{SnMe}_2\text{Cl})]$.²³ These differences are consistent with the substantial (but not complete) reduction in the multiplicity of the M–P bond operated upon formation of our neutral oxophosphinidene complexes, a matter discussed above on the basis of the structural data for the lead complex **8**.

Interconversion Between Isomers 9 and 10. The reaction of **1** with SnMe_3Cl in tetrahydrofuran (THF) solution is not complete but reaches to an equilibrium point (eq 1) that can be shifted to the product side by removal of the solvent and extraction of the crude reaction mixture with petroleum ether.



Spectroscopic data recorded at room temperature for the neutral product obtained in this way (Table 1 and Experimental Section) indicate that it exists mainly in its oxophosphinidene-bridged form $[\text{MoCp}\{\text{P}(\text{OSnMe}_3)\text{R}^*\}(\text{CO})_2]$ (**9**), these being comparable to those of the GePh_3 product **4**. However, the considerable broadness of the corresponding ¹H and ³¹P NMR resonances at room temperature suggested the occurrence of dynamic processes in solution. Indeed, upon cooling a CD_2Cl_2 solution of this compound, the broad ³¹P resonance observed at about 370 ppm at room temperature further broadens and eventually splits, so that at 243 K two broad resonances at 359.3 and 458.0 ppm are clearly defined, with relative intensities about 2:1, which we assign respectively to the isomers **9** and **10** on the basis of their spectroscopic properties and analogies with the complexes **2** to **8**. Further cooling of the solution increases the relative amount of the more deshielded resonance, so that below 203 K only the resonance due to the isomer **10** is present in

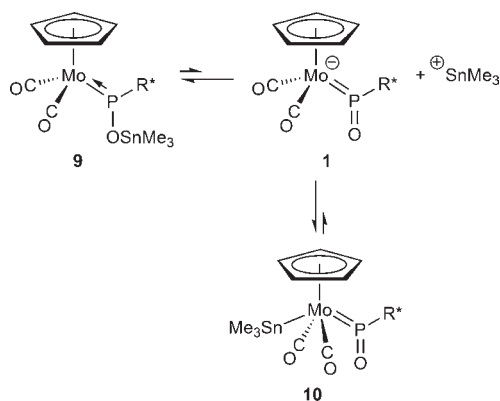
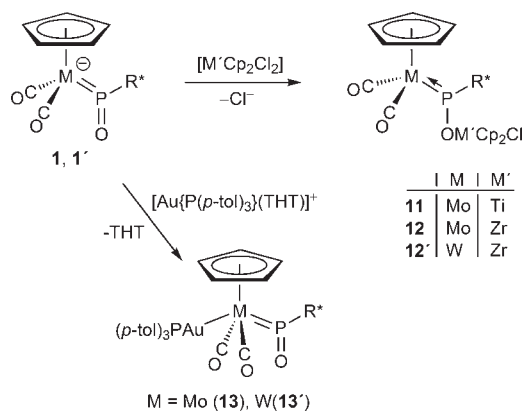
(19) Bala, M. D.; Leventis, D. C.; Coville, N. J. *J. Organomet. Chem.* **2006**, *691*, 1919, and references therein.

(20) Faller, J. W.; Anderson, A. S. *J. Am. Chem. Soc.* **1970**, *92*, 5852.

(21) (a) Nakazawa, H.; Kishishita, M.; Ishiyama, T.; Mizuta, T.; Miyoshi, K. *J. Organomet. Chem.* **2001**, *617*, 453. (b) Nakazawa, H.; Kishishita, M.; Yoshinaga, S.; Yamaguchi, Y.; Mizuta, T.; Miyoshi, K. *J. Organomet. Chem.* **1997**, *529*, 423.

(22) Smith, J. M.; Coville, N. J.; Cook, L. M.; Boeyens, J. C. A. *Organometallics* **2000**, *19*, 5273.

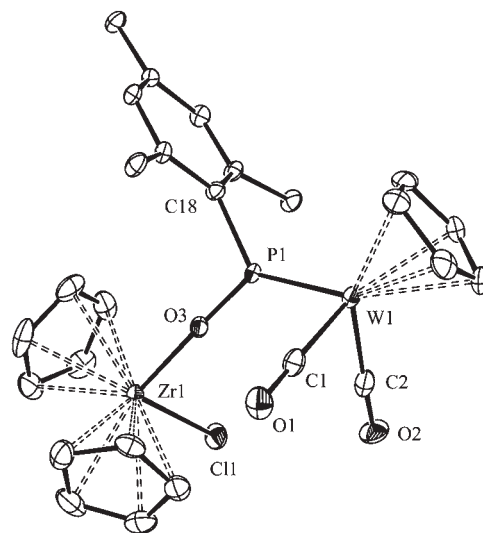
(23) Braunschweig, H.; Bera, H.; Geibel, B.; Dörfler, R.; Götz, D.; Seeler, F.; Kupfer, T.; Radacki, K. *Eur. J. Inorg. Chem.* **2007**, 3416.

Scheme 3. Dissociative Isomerization Proposed for Compound **9** in Solution**Scheme 4**

the ^{31}P NMR spectrum. From these data we conclude that isomers **9** and **10** interconvert rapidly in solution, and that at room temperature there is only a tiny amount of isomer **10** in equilibrium with the major, phosphide-like isomer **9**. The equilibrium observed in the synthesis of this compound in THF solutions (eq 1) suggests that the interconversion between isomers **9** and **10** in dichloromethane solutions also might be dissociative in nature, that is, with the intermediacy of a small amount of the anion **1** (Scheme 3). In agreement with this proposal, a separated experiment showed that compound **9** reacted with SnPh_3Cl in dichloromethane solution at room temperature to quantitatively give the SnPh_3 compound **6**.

Reactions of Compounds **1 and **1'** with Halide Metal Complexes.** The anionic complexes **1** and **1'** react readily with different halide complexes of the transition and post-transition elements such as the group 4 metallocene chlorides $[\text{M}'\text{Cp}_2\text{Cl}_2]$, and gold(I) complexes of the type $[\text{AuCl}(\text{PR}_3)]$. Other halocomplexes having more covalent M–X bonds such as the carbonylic complexes $[\text{MoClCp}(\text{CO})_3]$, $[\text{MBr}(\text{CO})_3]$ (M = Mn, Re), and $[\text{FeCpCl}(\text{CO})_2]$ failed to react with the molybdenum compound **1** in dichloromethane or THF solutions. Once again, the fragments arising from the halide metal complexes can bind either the oxygen atom of the oxophosphinidene ligand or the metal atom of the anion, depending on the reagent being used (Scheme 4).

Thus the reactions with stoichiometric amounts of $[\text{M}'\text{Cp}_2\text{Cl}_2]$ ($\text{M}' = \text{Ti}, \text{Zr}$) give the corresponding oxophosphinidene-bridged complexes $[\text{MoCp}\{\text{P}(\text{OTiCp}_2\text{Cl})\text{R}^*\}(\text{CO})_2]$ (**11**),

**Figure 2.** ORTEP drawing (30% probability) of the molecular structure of compound **12'**, with all H atoms and Me groups omitted for clarity.**Table 3.** Selected Bond Lengths (Å) and Angles (deg) in Compound **12'**

W(1)–C(1)	1.947(7)	Zr(1)–O(3)	2.016(4)
W(1)–C(2)	1.954(7)	P(1)–O(3)	1.563(4)
W(1)–P(1)	2.233(1)	P(1)–C(18)	1.851(5)
C(1)–W(1)–C(2)	84.7(3)	O(3)–P(1)–C(18)	100.1(2)
C(1)–W(1)–P(1)	90.3(2)	O(3)–P(1)–W(1)	127.4(2)
C(2)–W(1)–P(1)	89.3(2)	C(18)–P(1)–W(1)	132.4(2)
P(1)–O(3)–Zr(1)	177.7(2)		

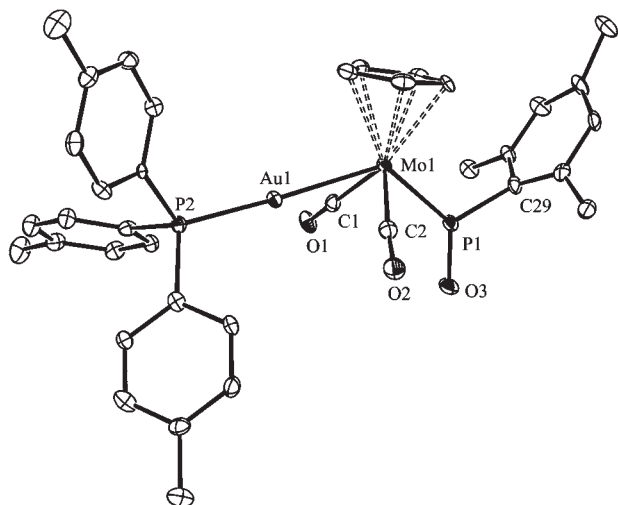
$[\text{MoCp}\{\text{P}(\text{OZrCp}_2\text{Cl})\text{R}^*\}(\text{CO})_2]$ (**12**), and $[\text{WCp}\{\text{P}(\text{OZrCp}_2\text{Cl})\text{R}^*\}(\text{CO})_2]$ (**12'**). In contrast, the anions **1** and **1'** react with $[\text{AuCl}\{\text{P}(p\text{-tol})_3\}]$ to give metal–metal bonded compounds. In this case, the reaction gives the corresponding oxophosphinidene complexes $[\text{MCp}\{\text{P}(\text{O})\text{R}^*\}(\text{CO})_2\{\text{AuP}(p\text{-tol})_3\}]$ [M = Mo (**13**), W(**13'**)], but an equilibrium is reached when using THF as solvent, and these products actually are more conveniently prepared by reacting the tetrahydrothiophene complex $[\text{Au}\{\text{P}(p\text{-tol})_3\}(\text{THT})][\text{PF}_6]$ in the same solvent. Attempts to prepare a related MoAg species using $[\text{AgCl}(\text{PPh}_3)]$ were unsuccessful, but the reaction of **1** with the perchlorate complex $[\text{Ag}(\text{ClO}_4)(\text{PPh}_3)]$ gave a product tentatively formulated as the corresponding oxophosphinidene derivative $[\text{MoCp}\{\text{P}(\text{O})\text{R}^*\}(\text{CO})_2\{\text{Ag}(\text{PPh}_3)\}]$ on the basis of its spectroscopic similarities ($\nu(\text{CO})$ 1880 (m), 1815 (vs) cm^{-1} , $\delta_{\text{P}} = 428$ ppm) with the gold complex **13**. However, attempts to isolate this unstable product as a reasonably pure solid were unsuccessful.

We should remark that the heterometallic compounds **11** and **12** are (along with **9**) almost the first complexes reported to have an oxophosphinidene ligand bridging two metal atoms in a $\mu_2\text{-P,O}$ fashion, the only precedent being found in the MoZr complex $[\text{Mo}\{\text{NR}(\text{Ar})\}_3\text{-}\{\text{P}(\text{OM})\text{Me}\}]$ (M = ZrCp₂Me).^{4d} Since a $[\text{M}'\text{Cp}_2\text{Cl}]^+$ ($\text{M}' = \text{Ti}, \text{Zr}$) fragment can be considered as a hard electrophile because of the high oxidation state of the metal atom, then it is not surprising that such a fragment ended up bound to the O atom of the oxophosphinidene ligand, because this is the expected result under conditions of charge control, as discussed above. In contrast, the $[\text{Au}\{\text{P}(p\text{-tol})_3\}]^+$ fragment can be considered as a much

Table 4. IR and $^{31}\text{P}\{^1\text{H}\}$ NMR Data for Compounds **11**–**13**

compound	$\nu_{\text{st}}(\text{CO})^a/\text{cm}^{-1}$	$\delta_{\text{P}}/\text{ppm}^b$ [J/Hz]
$[\text{MoCp}\{\text{P}(\text{OTiCp}_2\text{Cl})\text{R}^*\}(\text{CO})_2]$ (11)	1915 (vs), 1839 (s)	361.6
$[\text{MoCp}\{\text{P}(\text{OZrCp}_2\text{Cl})\text{R}^*\}(\text{CO})_2]$ (12)	1921 (vs), 1841 (s)	350.3
$[\text{WCp}\{\text{P}(\text{OZrCp}_2\text{Cl})\text{R}^*\}(\text{CO})_2]$ (12')	1913 (vs), 1830 (s)	303.7 [$J_{\text{PW}} = 724$]
$[\text{MoCp}\{\text{P}(\text{O})\text{R}^*\}(\text{CO})_2\{\text{AuP}(p\text{-tol})_3\}]$ (13)	1896 (m), 1840 (vs)	443.6 (s, br), 48.4 [d, $J_{\text{PP}} = 8$, AuP] ^c
$[\text{WCp}\{\text{P}(\text{O})\text{R}^*\}(\text{CO})_2\{\text{AuP}(p\text{-tol})_3\}]$ (13')	1897 (m), 1835 (vs)	393.2 [s, br, $J_{\text{PW}} = 530$], 54.9 [d, $J_{\text{PP}} = 10$, AuP]

^a Recorded in dichloromethane solution, unless otherwise stated. ^b Recorded in CD_2Cl_2 solution at 290 K and 121.50 MHz unless otherwise stated; δ relative to external 85% aqueous H_3PO_4 . ^c Recorded at 81.03 MHz.

**Figure 3.** ORTEP drawing (30% probability) of the molecular structure of compound **13**, with all H atoms and Me groups (except those of the *p*-tol rings) omitted for clarity.

softer acid, and therefore should interact with the anions **1** and **1'** under the driving force of the more favorable orbital interactions. Hence, a metal–metal bonded product is more likely to be formed, as observed in the reactions with the tin and lead organohalides.

Structural Characterization of Compounds **11** and **12**.

The molecule of the WZr complex **12'** in the crystal (Figure 2 and Table 3) is made up from $\text{WCp}(\text{CO})_2$ and ZrCp_2Cl fragments bridged by an oxophosphinidene ligand through its P and O atoms, respectively. The coordination geometry around tungsten is of the classical tree-legged piano stool type, actually very similar to that of the fluoro- and alkoxyphosphide derivatives of **1** previously reported by us ($[\text{MoCp}(\text{PXR}^*)(\text{CO})_2]$, with $\text{X} = \text{F}, \text{C}(\text{O})\text{Ph}$).⁶ In particular, the short W–P length of 2.233(1) Å and the planar geometry around phosphorus (sum of angles = 359.9°) is consistent with the formulation of a double W–P bond for this phosphide-like complex (cf. 2.239(1) Å for **1** or about 2.20 Å for the mentioned phosphide complexes). The P–O length of 1.563(4) Å is longer than those in the anion **1** (1.514(3) Å) or in the MoPb compound **8** (1.482(3) Å) as expected, but yet shorter than the single-bond P–O length measured in the mentioned alkoxyphosphide complex (1.661(4) Å),⁶ and even that in the related MoZr complex $[\text{Mo}\{\text{NR}(\text{Ar})\}_3\{\text{P}(\text{OZrCp}_2\text{Me})\text{Me}\}]$ (1.613(5) Å),^{4d} all of this suggesting the presence of some residual multiplicity in this formally single P–O bond of compound **12'**. Finally, the Zr–O length of 2.016(4) Å must be viewed as a normal figure for a single bond between these atoms (cf. 2.000(4) Å in the mentioned MoZr complex).

Table 5. Selected Bond Lengths (Å) and Angles (deg) in Compound **13**

Mo(1)–P(1)	2.289(2)	Mo(1)–C(1)	1.985(8)
Mo(1)–Au(1)	2.7071(7)	Mo(1)–C(2)	1.974(8)
Au(1)–P(2)	2.274(2)	P(1)–O(3)	1.498(5)
P(1)–C(29)	1.861(8)		
C(2)–Mo(1)–C(1)	99.4(3)	O(3)–P(1)–C(29)	114.5(3)
C(2)–Mo(1)–P(1)	82.3(2)	O(3)–P(1)–Mo(1)	130.4(2)
C(1)–Mo(1)–P(1)	80.7(2)	C(29)–P(1)–Mo(1)	115.1(2)
C(1)–Mo(1)–Au(1)	63.2(2)	O(1)–C(1)–Mo(1)	173.5(7)
C(2)–Mo(1)–Au(1)	67.0(2)	O(2)–C(2)–Mo(1)	175.4(7)
P(1)–Mo(1)–Au(1)	126.0(1)		

Spectroscopic data in solution for compounds **11**, **12**, and **12'** (Table 4) are similar to each other and consistent with the structure found for **12'** in the crystal. Moreover they are also comparable to those of the silicon and germanium compounds **2** to **5** (Table 2). Thus, their IR spectra also display two C–O stretching bands of strong intensity, although the frequencies are a bit lower than those of the Si and Ge compounds, an effect that can be attributed to the lower electron-withdrawing power of the group 4 elements. In apparent relationship with this, the ^{31}P resonances of these complexes are less shielded than those of the Si and Ge compounds, they appearing midway between the latter resonances and those of the starting anions **1** and **1'**. Yet, the P–W coupling in **12'** (724 Hz) has a magnitude comparable to the value measured for the silicon compound **2'** (735 Hz), significantly higher than that in the anion **1'** (658 Hz), and in any case consistent with the double M–P bonds that should be formulated for all these complexes, also substantiated by the short P–W length found in the crystal for **12'**.

Structural Characterization of Compounds **13** and **13'**.

The molecular structure of the molybdenum compound **13** in the crystal (Figure 3 and Table 5) displays a distorted four-legged piano stool structure very similar to that of the lead compound **8**, if we just replace the PbPh_3 group by a $\text{AuP}(p\text{-tol})_3$ one, with the latter conforming to a linear coordination geometry around the gold atom. The geometrical distortions around the Mo atom in **13** are very similar to those observed for **8** and need not to be discussed in detail, being reflected in comparable values for the angles defined by the ligands and the Cp centroid ($\text{Au–Mo–Cp}(\text{centr.}) = 110.1^\circ$, $\text{P–Mo–Cp}(\text{centr.}) = 123.8^\circ$), and the angles between ligands ($\text{C–Mo–C} = 99.4(3)^\circ$, $\text{Au–Mo–P} = 126.0(1)^\circ$).

The Mo–P (2.289(2) Å) and the P–O (1.498(5) Å) lengths in **13** are respectively slightly shorter and longer than the corresponding figures in the lead compound **8** (2.319(1) Å and 1.482(7) Å). This suggests the retention of a slightly higher multiplicity in the Mo–P bond for the gold compound, that might be attributed to the comparatively smaller reduction of electron density that occurred at the Mo site (and hence less reduction in the back-donation to

phosphorus) upon addition of the gold fragment. This is in agreement with the C–O stretching frequencies of the gold compounds, some 50 cm^{-1} lower than those of the corresponding lead compounds (see below).

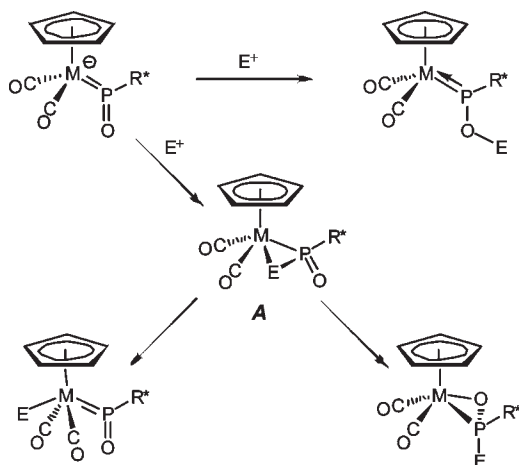
The Mo–Au length of $2.7071(7)\text{ \AA}$ in **13** is only marginally lower than the corresponding values in the related tricarbonyl complexes $[\text{MoCp}(\text{CO})_3\{\text{Au}(\text{PPh}_3)\}]$ ($2.710(1)\text{ \AA}$) and $[\text{Mo}(\eta^5\text{-C}_5\text{H}_4\text{CHO})(\text{CO})_3\{\text{Au}(\text{PPh}_3)\}]$ ($2.7121(5)\text{ \AA}$).²⁴ From this we conclude once again that the *trans* influence of the oxophosphinidene ligand is of comparable magnitude to that of a carbonyl ligand. We finally notice the relatively close approach of the carbonyl ligands to the gold atom in **13** ($\text{Au}\cdots\text{C}$ separations of $2.533(8)$ and $2.654(8)\text{ \AA}$), a feature relatively common in mono and polynuclear carbonyl complexes of the transition metals having AuPR_3 fragments (e.g., $\text{Au}\cdots\text{C}$ ca. 2.49 \AA in $[\text{Mo}(\text{BnN}^i\text{Pr}_2)(\text{CO})_3\{\text{Au}(\text{PPh}_3)\}]$, $\text{Bn} = \eta^5\text{-C}_{10}\text{H}_9\text{B}$).²⁵ We trust there are no genuine bonding interactions in the case of **13**, not just because of the linearity of these carbonyl ligands but also because almost identical positions of the carbonyl ligands are observed for the lead compound **8**, although the larger intermetallic separation in that case (ca. 2.9 \AA) also implies larger and clearly nonbonding $\text{Pb}\cdots\text{C}(\text{O})$ separations of about 2.9 \AA .

Spectroscopic data in solution for **13** and **13'** are comparable to each other and consistent with the *trans*-dicarbonyl structure found for the molybdenum compound in the crystal. The C–O stretching frequencies are some 50 cm^{-1} lower than those of the corresponding Pb compounds of type **8**, this being explained by taking into consideration the great difference in the oxidation states of the metal atoms involved in each case (I vs IV). The electron density at the group 6 metal atom in compounds **13** therefore must be intermediate between these in the anions **1** and **1'** and those in the tin and lead compounds **6** to **8** and, according to the discussion made above for the latter compounds, the diamagnetic contribution to the shielding of the ^{31}P nucleus would have also an intermediate magnitude. In agreement with this, the ^{31}P resonance in compounds **13** appears some 60 ppm higher than in corresponding anion, but still some 20 ppm lower than those of the related tin and lead derivatives (Tables 2 and 4). Finally, the ^{31}P spectra of compounds **13** also display a much more shielded resonance corresponding to the gold-bound phosphine ligand, in a position (ca. 50 ppm) comparable to those observed for related MoAu compounds (e.g., 47.8 ppm for $[\text{Mo}(\text{BnN}^i\text{Pr}_2)(\text{CO})_3\{\text{Au}(\text{PPh}_3)\}]$,²⁵ or 47.7 ppm for $[\text{MoCp}(\text{CO})_2(\text{PMe}_3)\{\text{Au}(\text{PPh}_3)\}]$.²⁶

Concluding Remarks

The reactions of the anionic complexes **1** and **1'** with electrophilic halide compounds (E–Cl) of elements different from carbon bear some parallelism but also significant differences with the reactions of these anions with C-based electrophiles. Reagents based on hard and strong electron-withdrawing centers [Si(IV), Ge(IV), Ti(IV), Zr(IV)] end up

Scheme 5



bound to the oxygen atom of the oxophosphinidene ligand to give oxophosphinidene-bridged derivatives of the type $[\text{MCp}\{\text{P}(\text{OE})\text{R}^*\}(\text{CO})_2]$, thus resembling the reactions with strong C-based electrophiles to give alkoxyphosphide derivatives, as expected for interactions proceeding under conditions of charge control (Scheme 5). Reagents based on softer and milder electron-withdrawing centers [Sn(IV), Pb(IV), Au(I), Ag(I)] give instead metal–metal bonded products of the type $[\text{MCp}\{\text{P}(\text{O})\text{R}^*\}(\text{CO})_2(\text{E})]$ as a result of the attachment of the incoming electrophile to the metal site of the anion. This is in marked contrast with the reactivity of **1** toward mild C-based electrophiles, the latter resulting in the attachment of the incoming electrophile to the P atom of the oxophosphinidene ligand to yield a phosphinite derivate, as noted above (Scheme 1). These apparently divergent results might be considered as different evolutions of a common type of intermediate species by recalling that, according to the DFT calculations on **1**,⁶ the frontier orbitals in these anions have M–P π bonding character. Therefore, under conditions of orbital control (mild and soft electrophilic reagents) we should expect that a generic electrophile would interact initially with the M–P bond. The resulting intermediate species **A** might afterward rearrange in two different ways: either by a movement of the electrophilic fragment into a terminal position at phosphorus (route followed by the hydrocarbon electrophiles) or into a terminal position at the metal (route followed by the metallic electrophiles) (Scheme 5). A delicate balance among the different bonds being broken and formed seems to favor the formation of the E–P bonds only for the hydrocarbon fragments, but steric effects must be also operative, the latter disfavoring the attachment of the incoming electrophile at the quite congested P site. This might be a determinant factor in the case of the comparatively bulkier metallic fragments studied in the present work.

Upon attachment of an electrophile at the metal site (to give a terminal oxophosphinidene complex) there is a strong reduction of the electron density at that site and a significant reduction in the multiplicity of the M–P bond because of the concomitant reduction in the back-donation from M to P. As a result, the P nucleus of the oxophosphinidene ligand is significantly *deshielded*, and a plot of the ^{31}P chemical shifts for these complexes with respect to their average C–O stretching frequencies relative to the anion **1**

(24) Fischer, P. J.; Krohn, K. M.; Mwenda, E. T.; Young, V. G. *Organometallics* **2005**, *24*, 5116.

(25) Braunstein, P.; Cura, E.; Herberich, G. E. *J. Chem. Soc., Dalton Trans.* **2001**, 1754.

(26) Galassi, R.; Poli, R.; Alessandra, E.; Fettingner, J. C. *Inorg. Chem.* **1997**, *36*, 3001.

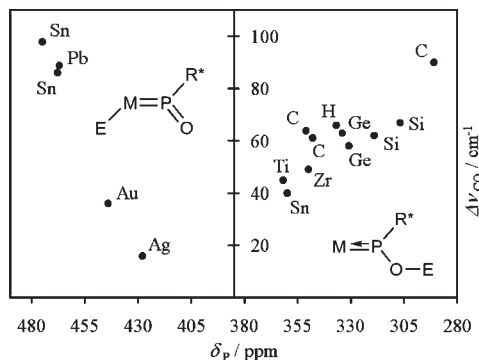


Figure 4. ^{31}P Chemical shifts (δ_{P} /ppm) for molybdenum complexes with terminal and bridging oxophosphinidene ligands, plotted against their average C–O stretching frequency relative to that of the anion **1** ($\Delta\nu_{\text{CO}}/\text{cm}^{-1}$), with the type of element (E) bound to O or Mo indicated in each case. The vertical axis is positioned at the chemical shift of the anion **1** (385 ppm). All data in CH_2Cl_2 or CD_2Cl_2 solutions and taken from this work and from reference 6.

(taken here as an indicator of electron density at the metal) reveals a good correlation although not a linear one, therefore suggesting that the overall reduction of the electron density at phosphorus (caused indirectly by the attachment of the electrophile at the metal site) must be one of the major factors governing the observed changes in the ^{31}P shifts (Figure 4). In contrast, the attachment of an electrophile at the O site of the anion to give an oxophosphinidene-bridged complex also implies a reduction (even if not so strong) of the electron density at the metal site, but now a reinforcement of the M–P bond. The latter can be explained by taking into account that the electron density removed from the metal is now being driven toward the P atom, therefore reinforcing the π component of the M–P bond. As a result of this electron redistribution the P nucleus of the oxophosphinidene ligand is significantly shielded, and a similar plot of the ^{31}P chemical shifts for the corresponding compounds (including the alkoxyphosphide complexes previously reported by us) reveals a gross correlation with respect to their average C–O stretching frequencies, although not as good as the one apparent for the terminal oxophosphinidene complexes.

Experimental Section

General Procedures and Starting Materials. All manipulations and reactions were carried out under a nitrogen (99.995%) atmosphere using standard Schlenk techniques. Solvents were purified according to literature procedures,²⁷ and distilled prior to use. Petroleum ether refers to that fraction distilling in the range 338–342 K. Compounds $(\text{H-DBU})[\text{MCp}(\text{CO})_2\{\text{P}(\text{O})\text{R}^*\}]$ (M = Mo (**1**), W (**1'**); DBU = 1,8-diazabicyclo [5.4.0] undec-7-ene; $\text{R}^* = 2,4,6\text{-C}_6\text{H}_2\text{tBu}_3$)⁶ and $[\text{AuCl}\{\text{P}(p\text{-tol})_3\}]$ ²⁸ were prepared as described previously. All other reagents were obtained from the usual commercial suppliers and used as received. Chromatographic separations were carried out using jacketed columns cooled by tap water (ca. 288 K). Commercial aluminum oxide (activity I, 150 mesh) was degassed under vacuum prior to use. The latter was mixed under nitrogen with the appropriate amount of water to reach the activity desired. Filtrations were performed using diatomaceous earth. IR stretching frequencies of CO ligands were measured typically in solution. Nuclear Magnetic Resonance (NMR) spectra were routinely recorded at

300.13 (^1H), 121.50 ($^{31}\text{P}\{^1\text{H}\}$), or 75.47 MHz ($^{13}\text{C}\{^1\text{H}\}$) at 290 K in CD_2Cl_2 solutions unless otherwise stated. Chemical shifts (δ) are given in ppm, relative to internal tetramethylsilane (TMS) or external 85% aqueous H_3PO_4 solutions (^{31}P). Coupling constants (J) are given in hertz (Hz).

Preparation of $[\text{MoCp}\{\text{P}(\text{OSiMe}_3)\text{R}^*\}(\text{CO})_2]$ (2**).** Neat SiMe_3Cl (14 μL , 0.108 mmol) was added to a dichloromethane solution (10 mL) of compound **1** (0.036 g, 0.054 mmol), whereupon the solution changed immediately from yellow to red. The solvent was then removed under vacuum, the residue was extracted with petroleum ether, and the extracts were filtered. Removal of the solvent from the filtrate yielded compound **2** as a red microcrystalline solid (0.026 g, 81%). Anal. Calcd for $\text{C}_{28}\text{H}_{43}\text{O}_3\text{MoPSi}$: C, 57.72; H, 7.44. Found: C, 57.32; H, 7.58. ^1H NMR (200.13 MHz): δ 7.36 (d, $J_{\text{HP}} = 3$, 2H, C_6H_2), 4.99 (s, 5H, Cp), 1.59 (s, 18H, $o\text{-}^t\text{Bu}$), 1.32 (s, 9H, $p\text{-}^t\text{Bu}$), 0.39 (s, 9H, SiMe).

Preparation of $[\text{WCp}\{\text{P}(\text{OSiMe}_3)\text{R}^*\}(\text{CO})_2]$ (2'**).** The procedure is completely analogous to that described for **2**, but now using compound **1'** (0.030 g, 0.040 mmol) and SiMe_3Cl (10 μL , 0.077 mmol). This yielded compound **2'** as a red microcrystalline solid (0.021 g, 78%). Anal. Calcd for $\text{C}_{28}\text{H}_{43}\text{O}_3\text{PSiW}$: C, 50.15; H, 6.46. Found: C, 50.22; H, 6.54. ^1H NMR (200.13 MHz): δ 7.37 (d, $J_{\text{HP}} = 3$, 2H, C_6H_2), 5.04 (s, 5H, Cp), 1.58 (s, 18H, $o\text{-}^t\text{Bu}$), 1.31 (s, 9H, $p\text{-}^t\text{Bu}$), 0.40 (s, 9H, SiMe).

Preparation of $[\text{MoCp}\{\text{P}(\text{OSiPh}_3)\text{R}^*\}(\text{CO})_2]$ (3**).** Solid SiPh_3Cl (0.025 g, 0.082 mmol) was added to a dichloromethane solution (10 mL) of compound **1** (0.036 g, 0.054 mmol) whereupon the solution changed immediately from yellow to red. The solvent was then removed under vacuum, the residue was washed with petroleum ether (2×4 mL) and then extracted with diethyl ether. Removal of the solvent from the filtered extracts yielded compound **3** as a red solid (0.033 g, 79%). Anal. Calcd for $\text{C}_{43}\text{H}_{49}\text{O}_3\text{MoPSi}$: C, 67.17; H, 6.42. Found: C, 67.02; H, 6.49. ^1H NMR (200.13 MHz): δ 7.64–7.30 (m, 6H, Ph), 7.48–7.30 (m, 11H, Ph and C_6H_2), 5.03 (s, 5H, Cp), 1.49 (s, 18H, $o\text{-}^t\text{Bu}$), 1.34 (s, 9H, $p\text{-}^t\text{Bu}$).

Preparation of $[\text{MoCp}\{\text{P}(\text{OGePh}_3)\text{R}^*\}(\text{CO})_2]$ (4**).** Solid GePh_3Br (0.018 g, 0.045 mmol) was added to a dichloromethane solution (10 mL) of compound **1** (0.030 g, 0.045 mmol), and the mixture was stirred at 273 K for 10 min to give an orange solution. Workup as described for **2** (filtration using a canula) gave compound **4** as an orange, quite air-sensitive solid (0.031 g, 84%). ^1H NMR: δ 7.74–7.59 (m, 6H, Ph), 7.53–7.38 (m, 9H, Ph), 7.34 (s, 2H, C_6H_2), 4.88 (s, 5H, Cp), 1.51 (s, 18H, $o\text{-}^t\text{Bu}$), 1.32 (s, 9H, $p\text{-}^t\text{Bu}$).

Preparation of $[\text{MoCp}\{\text{P}(\text{OGeMe}_2\text{Cl})\text{R}^*\}(\text{CO})_2]$ (5**).** The procedure is completely analogous to that described for compound **4**, but now using GeMe_2Cl_2 (0.008 g, 0.046 mmol) and a reaction time of 1 min. This yielded compound **5** as an orange, quite air-sensitive solid (0.023 g, 79%). ^1H NMR (200.13 MHz): δ 7.32 (s, 2H, C_6H_2), 4.96 (s, 5H, Cp), 1.56 (s, 18H, $o\text{-}^t\text{Bu}$), 1.32 (s, 6H, GeMe), 1.29 (s, 9H, $p\text{-}^t\text{Bu}$).

Preparation of $[\text{MoCp}\{\text{P}(\text{O})\text{R}^*\}(\text{CO})_2(\text{SnPh}_3)]$ (6**).** Solid SnPh_3Cl (0.037 g, 0.096 mmol) was added to a dichloromethane solution (10 mL) of compound **1** (0.030 g, 0.045 mmol), and the mixture was stirred for 1 min to give a pale yellow solution. The solvent was then removed under vacuum, the residue was extracted with toluene, and the extracts were filtered using a canula. Crystallization of the filtrate from toluene-petroleum ether (1:2) gave compound **6** as a yellow microcrystalline solid (0.035 g, 90%). Anal. Calcd for $\text{C}_{43}\text{H}_{49}\text{O}_3\text{MoPSn}$: C, 60.09; H, 5.75. Found: C, 60.40; H, 5.90. $\nu(\text{P}=\text{O})$ (Nujol mull) 1184 cm^{-1} . ^1H NMR (200.13 MHz): δ 7.58–7.34 (m, 17H, Ph and C_6H_2), 4.82 (s, 5H, Cp), 1.64 (s, 18H, $o\text{-}^t\text{Bu}$), 1.35 (s, 9H, $p\text{-}^t\text{Bu}$).

Preparation of $[\text{MoCp}\{\text{P}(\text{O})\text{R}^*\}(\text{CO})_2(\text{SnPh}_2\text{Cl})]$ (7**).** Solid SnPh_2Cl_2 (0.017 g, 0.048 mmol) was added to a stirred dichloromethane solution (10 mL) of compound **1** (0.030 g, 0.045 mmol) at 273 K to rapidly give a pale yellow solution. The solvent was then removed under vacuum, the residue was extracted with toluene-petroleum ether (1:2), and the extract was filtered using

(27) Perrin, D. D.; Armarego, W. L. F. *Purification of Laboratory Chemicals*; Pergamon Press: Oxford, U. K., 1988.

(28) Braunstein, P.; Lehrer, H.; Matt, D. *Inorg. Synth.* **1990**, 218.

a canula. Removal of the solvents from the filtrate gave complex **7** as a yellow powder (0.032 g, 86%). Anal. Calcd for $C_{37}H_{44}O_3ClMoPSn$: C, 54.34; H, 5.42. Found: C, 54.65; H, 5.54. 1H NMR: δ 8.10 (m, 1H, C_6H_2 , *cis* isomer), 7.95 (m, 1H, C_6H_2 , *cis* isomer), 7.68 (m, 4H, Ph, *trans* isomer), 7.50–7.38 (m, Ph, *cis* isomer, and Ph and C_6H_2 , *trans* isomer), 5.26 (s, 5H, Cp, *cis* isomer), 4.96 (s, 5H, Cp, *trans* isomer), 1.64 (s, 18H, *o*-^tBu, *trans* isomer), 1.61 (s, 9H, CH_3 *cis* isomer), 1.35 (s, 9H, *p*-^tBu *trans* isomer), 1.28 (s, 9H, CH_3 , *cis* isomer), 1.17 (s, 9H, CH_3 , *cis* isomer), (ratio *trans/cis* = 3.5). $^{119}Sn\{^1H\}$ NMR: δ 216.9 [d, J_{119SnP} = 149 Hz, *trans* isomer].

Preparation of $[WCp\{P(O)R^*\}(CO)_2(SnPh_2Cl)]$ (7'**).** The procedure is completely analogous to that described for compound **7**, but now using compound **1'** (0.030 g, 0.040 mmol) and $SnPh_2Cl_2$ (0.015 g, 0.042 mmol). This yielded compound **7'** as a yellow powder (0.030 g, 83%). Anal. Calcd for $C_{37}H_{44}O_3ClPSnW$: C, 49.07; H, 4.90. Found: C, 49.14; H, 5.09. 1H NMR: δ 8.07 (m, 1H, C_6H_2 , *cis* isomer), 7.91 (m, 1H, C_6H_2 , *cis* isomer), 7.67–7.30 (m, Ph, *cis* isomer, and Ph and C_6H_2 , *trans* isomer), 5.34 (s, 5H, Cp, *cis* isomer), 5.04 (s, 5H, Cp, *trans* isomer), 1.63 (s, 18H, *o*-^tBu, *trans* isomer), 1.61 (s, 9H, CH_3 *cis* isomer), 1.35 (s, 9H, *p*-^tBu, *trans* isomer), 1.28 (s, 9H, CH_3 , *cis* isomer), 1.19 (s, 9H, CH_3 , *cis* isomer), (ratio *trans/cis* = 3.5).

Preparation of $[MoCp\{P(O)R^*\}(CO)_2(PbPh_3)]$ (8**).** The procedure is completely analogous to that described for compound **7**, but now using $PbPh_3Cl$ (0.024 g, 0.045 mmol) and a toluene-petroleum ether (2:1) mixture for extractions. This yielded compound **8** as a yellow powder (0.039 g, 91%). The crystals used in the X-ray study were grown by slow diffusion of a layer of petroleum ether into a concentrated toluene solution of the complex at 253 K. Anal. Calcd for $C_{43}H_{49}O_3MoPpb$: C, 54.48; H, 5.21. Found: C, 54.12; H, 5.38. 1H NMR (200.13 MHz): δ 7.56–7.30 (m, 17H, Ph and C_6H_2), 4.86 (s, 5H, Cp), 1.65 (s, 18H, *o*-^tBu), 1.34 (s, 9H, *p*-^tBu).

Preparation of $[WCp\{P(O)R^*\}(CO)_2(PbPh_3)]$ (8'**).** The procedure is completely analogous to that described for compound **7**, but now using compound **1'** (0.030 g, 0.040 mmol) and $PbPh_3Cl$ (0.021 g, 0.040 mmol), and a toluene-petroleum ether (2:1) mixture for extractions. This yielded compound **8'** as a yellow powder (0.037 g, 90%). Anal. Calcd for $C_{43}H_{49}O_3PPbW$: C, 49.86; H, 4.77. Found: C, 49.74; H, 4.89. 1H NMR (200.13 MHz): δ 7.58–7.26 (m, 17H, C_6H_2 , Ph), 4.94 (s, 5H, Cp), 1.64 (s, 18H, *o*-^tBu), 1.34 (s, 9H, *p*-^tBu).

Preparation of $[MoCp\{P(OSnMe_3)R^*\}(CO)_2]$ (9**).** A large excess of $SnMe_3Cl$ (0.108 g, 0.54 mmol) was added to a stirred dichloromethane solution (10 mL) of compound **1** (0.036 g, 0.054 mmol), whereupon the solution changed immediately from yellow to orange. The solvent was then removed under vacuum, the residue was extracted with petroleum ether, and the extracts were filtered. Crystallization of the concentrated filtrate at 253 K yielded compound **9** as an orange microcrystalline solid (0.030 g, 81%). Anal. Calcd for $C_{28}H_{43}O_3MoPSn$: C, 49.95; H, 6.44. Found: C, 50.13; H, 6.58. 1H NMR (200.13 MHz, C_6D_6): Isomer **9**: δ 7.40 (s, 2H, C_6H_2), 4.87 (s, 5H, Cp), 1.68 (s, 18H, *o*-^tBu), 1.25 (s, 9H, *p*-^tBu), 0.40 (s, br, 9H, SnMe). 1H NMR (CD_2Cl_2 , 203K): Isomer **10**: δ 7.44 (s, 2H, C_6H_2), 4.87 (s, 5H, Cp), 1.68 (s, 18H, *o*-^tBu), 1.25 (s, 9H, *p*-^tBu), 0.40 (s, br, 9H, CH_3).

Preparation of $[MoCp\{P(OTiCp_2Cl)R^*\}(CO)_2]$ (11**).** Solid $[TiCp_2Cl_2]$ (0.014 g, 0.056 mmol) was added to a dichloromethane solution (10 mL) of compound **1** (0.036 g, 0.054 mmol), and the mixture was stirred for 2.5 h to give a red solution. The solvent was then removed under vacuum, the residue was extracted with petroleum ether, and the extracts were filtered. Removal of the solvents from the filtrate gave complex **11** as a red, quite air-sensitive powder (0.035 g, 90%). 1H NMR: δ 7.39 (d, J_{HP} = 2, 2H, C_6H_2), 6.51 (s, 10H, Cp), 5.04 (s, 5H, Cp), 1.63 (s, 18H, *o*-^tBu), 1.32 (s, 9H, *p*-^tBu).

Preparation of $[MoCp\{P(OZrCp_2Cl)R^*\}(CO)_2]$ (12**).** Solid $[ZrCp_2Cl_2]$ (0.019 g, 0.065 mmol) was added to a dichloromethane

solution (10 mL) of compound **1** (0.042 g, 0.063 mmol), and the mixture was stirred for 1 min to give a red solution. The solvent was then removed under vacuum, the residue was extracted with toluene, and the extracts were filtered. Removal of the solvent from the filtrate gave complex **12** as a red powder (0.045 g, 92%). Anal. Calcd for $C_{35}H_{44}O_3ClMoPZr$: C, 54.86; H, 5.79. Found: C, 55.10; H, 5.93. 1H NMR: δ 7.41 (d, J_{HP} = 2, 2H, C_6H_2), 6.39 (s, 10H, Cp), 5.12 (s, 5H, Cp), 1.65 (s, 18H, *o*-^tBu), 1.31 (s, 9H, *p*-^tBu).

Preparation of $[WCp\{P(OZrCp_2Cl)R^*\}(CO)_2]$ (12'**).** Solid $[ZrCp_2Cl_2]$ (0.017 g, 0.058 mmol) was added to a dichloromethane solution (10 mL) of compound **1'** (0.042 g, 0.056 mmol), and the mixture was stirred for 1 min to give a red solution. The solvent was then removed under vacuum, the residue was extracted with toluene-petroleum ether (2:1), and the extracts were filtered. Removal of the solvents from the filtrate gave compound **12'** as a red powder (0.042 g, 87%). The crystals used in the X-ray study were grown by slow diffusion of layers of petroleum ether and toluene into a concentrated CH_2Cl_2 solution of the complex at 253 K. Anal. Calcd for $C_{35}H_{44}O_3ClPWZr$: C, 49.21; H, 5.19. Found: C, 48.93; H, 5.08. 1H NMR: δ 7.41 (d, J_{HP} = 2, 2H, C_6H_2), 6.42 (s, 10H, Cp), 5.15 (s, 5H, Cp), 1.64 (s, 18H, *o*-^tBu), 1.31 (s, 9H, *p*-^tBu).

Preparation of $[MoCp\{P(O)R^*\}(CO)_2\{AuP(p-tol)_3\}]$ (13**).** A THF solution (5 mL) of $[Au\{P(p-tol)_3\}(THT)]PF_6$ was prepared in situ by stirring $[AuCl\{P(p-tol)_3\}]$ (0.016 g, 0.030 mmol) and $TIPF_6$ (0.010 g, 0.030 mmol) in the presence of THT (tetrahydrothiophen, 0.05 mL, excess) for 10 min. The solution was filtered using a canula and then cooled at 273 K and added to a THF solution (10 mL) of compound **1** (0.020 g, 0.030 mmol), and the mixture was stirred at 273 K for 1 min to give a pale-yellow solution. The solvent was then removed under vacuum, the residue was extracted with toluene-petroleum ether (2:1), and the extracts were filtered using a canula. Removal of the solvents from the filtrate gave complex **13** as a yellow powder (0.027 g, 90%). The crystals used in the X-ray study were grown by the slow diffusion of layers of petroleum ether and toluene into a concentrated CH_2Cl_2 solution of the complex at 253 K. Anal. Calcd for $C_{35}H_{44}O_3AuMoP$: C, 56.39; H, 5.66. Found: C, 56.08; H, 5.48. 1H NMR (200.13 MHz): δ 7.45–7.23 (m, 14H, C_6H_4 and C_6H_2), 4.93 (s, 5H, Cp), 2.39 (s, 9H, CH_3), 1.62 (s, 18H, *o*-^tBu), 1.34 (s, 9H, *p*-^tBu).

Preparation of $[WCp\{P(O)R^*\}(CO)_2\{AuP(p-tol)_3\}]$ (13'**).** The procedure is completely analogous to that described for compound **13**, but now using compound **1'** (0.020 g, 0.026 mmol). This yielded complex **13'** as a yellow powder (0.026 g, 90%). Anal. Calcd for $C_{35}H_{44}O_3AuPW$: C, 51.75; H, 5.19. Found: C, 52.02; H, 5.39. 1H NMR: δ 7.45–7.23 (m, 8H, C_6H_4 and C_6H_2), 7.25 (m, 6H, C_6H_4), 5.02 (s, 5H, Cp), 2.38 (s, 9H, CH_3), 1.60 (s, 18H, *o*-^tBu), 1.33 (s, 9H, *p*-^tBu).

X-ray Structure Determination for Compound 8. A single crystal was coated in paraffin oil and mounted on a glass fiber. X-ray measurements were made using a Bruker SMART CCD area-detector diffractometer with Mo-K α radiation.²⁹ Intensities were integrated from several series of exposures,³⁰ each exposure covering 0.3° in ω , and the total data set being a sphere. Absorption corrections were applied, based on multiple and symmetry-equivalent measurements.³¹ The structure was solved by direct methods and refined by least-squares on weighted F^2 values for all reflections (Table 6).³² All non-hydrogen atoms were assigned anisotropic displacement parameters and refined

(29) SMART Diffractometer Control Software; Bruker Analytical X-ray Instruments Inc.: Madison, WI, 1998.

(30) SAINT integration software; Siemens Analytical X-ray Instruments Inc.: Madison, WI, 1994.

(31) Sheldrick, G. M. SADABS, Program for Empirical Absorption Correction; University of Göttingen: Göttingen, Germany, 1996.

(32) SHELXTL program system, version 5.1; Bruker Analytical X-ray Instruments Inc.: Madison, WI, 1998.

Table 6. Crystal Data for Compounds 8, 12', 13

	8·1/2C ₇ H ₈	12'	13
mol formula	C _{46.5} H ₅₃ MoO ₃ PPb	C ₃₅ H ₄₄ ClO ₃ PWZr	C ₄₆ H ₅₅ AuMoO ₃ P ₂
mol wt	993.99	854.19	1010.75
cryst syst	monoclinic	monoclinic	monoclinic
space group	C2/c	P2 ₁ /c	P2 ₁ /c
radiation (λ, Å)	0.71073	1.54184	0.71073
a, Å	55.0030(14)	11.1396(3)	10.01660(10)
b, Å	10.2300(3)	17.1725(3)	26.9633(4)
c, Å	15.0932(4)	18.0948(3)	17.1911(4)
α, deg	90	90	90
β, deg	91.1580(10)	98.2870(10)	110.9870(10)
γ, deg	90	90	90
V, Å ³	8490.9(4)	3425.30(12)	4334.97(13)
Z	8	4	4
calcd density, gcm ⁻³	1.555	1.656	1.549
absorpt. coeff., mm ⁻¹	4.332	10.020	3.781
temperature, K	173(2)	150(2)	100(2) K
θ range (°)	2.02 to 27.46	3.57 to 69.80	1.48 to 25.24
index ranges (h, k, l)	-71/71; -13/13; -19/19	-13/13; 0/20; 0/21	-12/11; -32/0; -20/10
no. of reflns collected	43894	52614	20817
no. of indep reflns (R _{int})	9717 (0.0471)	6378(0.1258)	7525 (0.0383)
reflns with I > 2σ(I)	8223	5412	6081
R indexes ^a [data with I > 2σ(I)]	R ₁ = 0.0315, wR ₂ = 0.0762 ^b	R ₁ = 0.0510, wR ₂ = 0.1311 ^c	R ₁ = 0.0404, wR ₂ = 0.1085 ^d
R indexes ^a (all data)	R ₁ = 0.0416, wR ₂ = 0.0806 ^b	R ₁ = 0.0596, wR ₂ = 0.1453 ^c	R ₁ = 0.0588, wR ₂ = 0.1498 ^d
GOF	1.034	1.057	1.248
no. of restraints/params	227/549	0/388	0/490
Δρ(max, min), e Å ⁻³	1.827, -1.064	2.521, -1.196	1.497, -2.319

^a $R = \sum ||F_o| - |F_c|| / \sum |F_o|$. $wR = [\sum w(F_o^2 - F_c^2)^2 / \sum w|F_o|^2]^{1/2}$. $w = 1/[\sigma^2(F_o^2) + (aP)^2 + bP]$ where $P = (F_o^2 + 2F_c^2)/3$. ^b $a = 0.0370$, $b = 29.0672$. ^c $a = 0.1054$, $b = 0.0000$. ^d $a = 0.0826$, $b = 4.0595$.

without positional constraints. All hydrogen atoms were constrained to ideal geometries and refined with fixed isotropic displacement parameters. Refinement proceeded smoothly to give the residuals shown in Table 6. Complex neutral-atom scattering factors were used.³³

X-ray Structure Determination for Compounds 12' and 13. Data collection for these compounds was performed on a Nonius Kappa CCD single diffractometer, using Cu-K_α (12') or graphite-monochromated Mo-K_α (13) radiation. Images were collected at 29 or 40 mm fixed crystal-detector distance, using the oscillation method, with 1.5° or 1° oscillation and 60 or 50 s exposure time per image, for compounds 12' or 13 respectively. Data collection strategy was calculated with the program Collect.³⁴ Data reduction and cell refinements were performed with the programs HKL Denzo and Scalepack.³⁵ Semiempirical absorption corrections were applied using the program

SORTAV.³⁶ Using the program suite WinGX,³⁷ the structure were solved by Patterson interpretation and phase expansion, and refined with full-matrix least-squares on F² with SHELXL97.³⁸ All non-hydrogen atoms were refined anisotropically. All hydrogen atoms were geometrically placed, and they were given an overall isotropic thermal parameter. Further details of the data collection and refinements are given in the Table 6.

Acknowledgment. We thank the DGI of Spain and the Consejería de Educación de Asturias for financial support (Projects CTQ2006-01207 and IB05-110), and the MEC of Spain for a grant (to M.A.).

Supporting Information Available: A CIF file containing the crystallographic data for the structural analysis of compounds 8, 12', and 13. This material is available free of charge via the Internet at <http://pubs.acs.org>.

(33) *International Tables for Crystallography*; Kluwer: Dordrecht, The Netherlands, 1992; Vol. C.

(34) *Collect*; Nonius BV: Delft, The Netherlands, 1997–2004.

(35) Otwinowski, Z.; Minor, W. *Methods Enzymol.* **1997**, *276*, 307.

(36) Blessing, R. H. *Acta Crystallogr., Sect. A* **1995**, *51*, 33.

(37) Farrugia, L. J. *J. Appl. Crystallogr.* **1999**, *32*, 837.

(38) Sheldrick, G. M. *Acta Crystallogr., Sect. A* **2008**, *64*, 112.